Microbiology (1998), **144**, 1051–1061 Printed in Great Britain

Growth of green sulphur bacteria in experimental benthic oxygen, sulphide, pH and light gradients

Olivier Pringault,[1]† Michael Kühl,[2] Rutger de Wit[1] and Pierre Caumette[1]

Author for correspondence: Olivier Pringault. Tel: +49 421 2028 630. Fax: +49 421 2028 580. e-mail: opringau@mpi-bremen.de

[1] Laboratoire d'Océanographie Biologique, Université Bordeaux I, CNRS-URA 197, 2 rue du Professor Jolyet, F-33120 Arcachon, France

[2] Max Planck Institut für Marine Mikrobiologie, Microsensor Research Group, Celsiusstr. 1, D-28359 Bremen, Germany

The green sulphur bacterium *Prosthecochloris aestuarii* (strain CE 2401) was cultured in a benthic gradient chamber to study its growth and photosynthetic activity in experimental gradients of oxygen, sulphide and light. An axenic biofilm was obtained within evenly inoculated artificial sediment after 5 weeks of incubation. The phototrophic biofilm was located 2·2–3·5 mm below the sediment surface, i.e. below the maximal penetration depth of oxygen, thus confirming that growth of *P. aestuarii* was restricted to strictly anoxic sediment layers. The activity was limited by the diffusive flux of sulphide, showing the role of molecular diffusion in growth of this benthic species. Scalar irradiance was attenuated strongly in the biofilm, with distinct attenuation maxima at 750 nm corresponding to bacteriochlorophyll *c* (Bchl *c*) absorption and at 800 nm corresponding to bacteriochlorophyll *a* (Bchl *a*) absorption. Using radiance attenuation data as a proxy for photopigment contents it was shown that the ratio Bchl *a*/Bchl *c* changed with depth. This indicates chromatic adaptation to changing light climates in the sediment. Total sulphide oxidation was estimated from the sulphide fluxes from below into the reaction zone. Measurements of sulphide oxidation as a function of scalar irradiance in the reaction zone showed that anoxygenic photosynthesis of the biofilm was saturated at a scalar irradiance (430–830 nm) >2 μmol photons m^{-2} s^{-1}.

Keywords: *Prosthecochloris aestuarii*, benthic gradient chamber, microsensors, photoadaptation, *P* vs *I* curve

INTRODUCTION

Phototrophic sulphur bacteria are frequently found in illuminated aquatic environments containing hydrogen sulphide (Van Gemerden & Mas, 1995). Their abundances are often related to the presence of a physicochemical stratification, which can develop in the water column or in the sediment. Thus, phototrophic sulphur bacteria thrive in stratified lakes, where they occupy the illuminated part of anoxic waters (Pfennig, 1989). Similarly, they are very common in the top few millimetres of shallow aquatic sediments, and particularly in microbial mats (Stal *et al*., 1985; Van Gemerden, 1993; Van Gemerden *et al*., 1989).

Among the phototrophic sulphur bacteria, the green sulphur bacteria exhibit an extreme sensitivity to molecular oxygen. They are obligate anaerobes, and growth is entirely inhibited in the presence of trace amounts of molecular oxygen (Van Gemerden & Mas, 1995). Green sulphur bacteria have a very high affinity for sulphide (K_s 0·0008–0·002 mmol l^{-1}) (Van Gemerden, 1984) and can tolerate and grow in the presence of high sulphide concentrations (5–10 mM), which are toxic for most purple sulphur bacteria (Brune, 1989; Van Gemerden, 1987). Moreover, green sulphur bacteria only need low light fluxes for maintenance and growth (Van Gemerden, 1980; Overmann & Pfennig, 1992). While purple sulphur bacteria often form a distinct layer in benthic microbial mats, prolific developments of green sulphur bacteria are less frequent, but multi-layered

†**Present address:** Max Planck Institut für Marine Mikrobiologie, Microsensor Research Group, Celsiusstr. 1, D-28359 Bremen, Germany.

Abbreviations: BChl, bacteriochlorophyll; Bphaeo, bacteriophaeophytin; BGC, benthic gradient chamber; FMO, Fenna–Mathews–Olson (protein); NIR, near-infrared; PAR, photosynthetically active radiation.

microbial mats have been described with the lowermost layer composed mainly of the green sulphur bacterium *Prosthecochloris* (Nicholson *et al*., 1987; Pierson *et al*., 1987, 1990).

In stratified sediment ecosystems such as microbial mats, bacterial activity is dependent on molecular diffusion (Van Gemerden, 1993). In combination with the high density of micro-organisms, this leads to formation of steep gradients of, for example, oxygen and sulphide (Van Gemerden, 1993). Radiant energy is strongly attenuated in microbial mats by intense scattering and absorption due to the presence of high pigment concentrations. Hence, the spectral composition, spatial distribution and intensity of the radiant flux change rapidly with depth (Kühl *et al*., 1994a). In spite of the paramount importance of the physicochemical gradients for the growth and activity of microorganisms in microbenthic environments, most ecophysiological studies with isolated strains from these environments have been performed in homogeneous liquid media. To study the ecology and physiology of phototrophic sulphur bacteria growing in gradients, a new tool, the benthic gradient chamber (BGC), was developed (Pringault *et al*., 1996). This new system permits the cultivation of axenic strains of sulphur bacteria on artificial sediments (e.g. sterile sand) within experimental gradients of oxygen, sulphide and light mimicking *in situ* conditions.

The aim of this study was to investigate the factors controlling growth and photosynthetic activity of the green sulphur bacterium *Prosthecochloris aestuarii* strain CE 2401 in sediments. Therefore, the organism was cultured in the BGC in which natural benthic conditions were simulated. An axenic biofilm of *P. aestuarii* developed during a 5 week incubation period. The depth location of the population was traced from radiance attenuation profiles. The rates of the metabolic processes were calculated from oxygen, sulphide, pH and light profiles, and their shifts during experimental light–dark shifts. The rate of sulphide oxidation was related to the total radiant flux available in the biofilm, i.e. the scalar irradiance.

METHODS

Bacterial strain. *Prosthecochloris aestuarii* strain CE 2401 was cultured in the BGC (see Pringault *et al*., 1996, for more details). This strain, from the Arcachon culture collection, is a nonmotile bacterium able to grow photolithotrophically with sulphide or elemental sulphur as electron donor. Growth does not occur with thiosulphate as an electron donor and is inhibited by sulphite. The strain is very sensitive to molecular oxygen, which inhibits its growth (Guyoneaud, 1996). During the assemblage of the BGC, the top centimetre of the sterile sand column was evenly inoculated with a small volume (10 ml) from a batch culture of *P. aestuarii* in the exponential growth phase, equivalent to an inoculum of approximately 0·7 mg biomass (dry weight).

Culture conditions. The design and experimental handling of the BGC have been described in detail by Pringault *et al*. (1996); its use in this paper is summarized below. The culturing device is composed of an artificial sediment core 45 mm long (internal diameter 40 mm) sandwiched between an upper oxic and a lower anoxic sulphide-containing chamber to generate opposing oxygen and sulphide gradients. The core was illuminated vertically from above to create a light gradient. The sediment consisted of fine sterile sand with a grain size of 125–250 μm (Merck). Transport of solutes through the sand core was exclusively due to molecular diffusion (Pringault *et al*., 1996).

The two media in the upper and lower chamber had a similar composition, comprising reconstituted sea water (Meer Salz) at a salinity of 35‰, NH_4Cl (5 mM), KH_2PO_4 (0·5 mM), the trace elements solution SL12B without EDTA (1 ml l^{-1}) (Pfennig & Trüper, 1992) and the vitamin solution V7 (1 ml l^{-1}) (Pfennig & Trüper, 1992). The medium in the upper chamber was oxic and permanently saturated with sterile air provided through an air-lift. The temperature and the salinity were kept constant during the incubation time at 20 °C and 35‰, respectively. Thus, the oxygen concentration in the overlying water was 230 μM (Garcia & Gordon, 1992). The medium in the lower chamber was anoxic, and prepared under a headspace of nitrogen. Na_2S was added to the medium, to a final concentration of 40 mM. Due to the large volume of the lower chamber (2400 ml) and the long diffusion path (45 mm), the sulphide losses due to diffusion through the sand core after 5 weeks of incubation were only 6% of the initial concentration. Thus, the lower chamber practically acted as a constant source.

The medium in the upper compartment was amended with 4 mM $NaHCO_3$ (final concentration). An equilibrium was rapidly established between this culture medium and the air provided by the air-lift, resulting in a stable pH of 8·2–8·3. In the lower medium, bicarbonate ($NaHCO_3$) was added to a final concentration of 80 mM concomitantly with the sulphide addition. This allowed for a complete oxidation of sulphide to sulphate by photolithotrophy, i.e. $2HCO_3^- + 1H_2S \rightarrow 2[CH_2O] + 1SO_4^{2-}$ (Pringault *et al*., 1996). The final pH in the lower chamber was 7·5–7·6. As a result, vertical gradients of pH and bicarbonate were established within the sediment core.

The BGC was illuminated from above by a collimated light beam from an incandescent lamp (Philips). The light regime was 16 h light/8 h dark. The scalar irradiance at the sediment surface was 800 μmol photons $m^{-2}\,s^{-1}$ for visible light (430–700 nm) and 2200 μmol photons $m^{-2}\,s^{-1}$ for near-infrared light (NIR: 700–1000 nm). Details of the light measurement are given below.

Microscale light measurements. Light measurements were performed with fibre-optic microprobes (scalar irradiance and field radiance microprobes) connected to a cooled optical spectral multichannel analyser (O-SMA; Kühl & Jørgensen, 1992a). The raw spectra were smoothed mathematically to suppress high-freqency noise, by applying a 'Blackman window' lowpass filtering algorithm with a cutoff frequency of 0·05 (Asystant$^+$ software; cf. Kühl & Jørgensen, 1992a).

The scalar irradiance microprobe consisted of an integrating sphere (70 μm diameter) fixed to the light-collecting end of a tapered optical fibre (Lassen *et al*., 1992). The scalar irradiance probe was inserted into the sand at a zenith angle of 150° relative to the incident light. The scalar irradiance measurements were wavelength- calibrated using the line spectra from Ne and Hg lamps. The spectral sensitivity of the detector system combined with the light microsensor was calibrated in

air using a spectral irradiance standard lamp (Oriel), as described by Ploug *et al.* (1993).

The field radiance microprobe was made of a single optical fibre with a tip diameter of 125 μm and a narrow and well-defined acceptance cone (numerical aperture 0·2) (Kühl & Jørgensen, 1992a). The acceptance half-angle was 11·5 ° in air and 8·6 ° in water (Kühl & Jørgensen, 1994). Depth profiles of backscattered radiance were measured at 150° zenith angle relative to the incident light by penetrating the sand from the surface in vertical steps of 0·1–0·5 mm.

Light calculations. Due to the concavity of the BGC walls, it was not possible to visually detect precisely when the probe touched the sediment surface. Therefore, the maxima of scalar irradiance and backscattered radiance were aligned with the sediment surface, which is in agreement with previous observations in sediments (Kühl & Jørgensen, 1994; Kühl *et al.*, 1994a; Lassen *et al.*, 1992).

The attenuation coefficient for backscattered field radiance, K_L, was calculated from profiles using a method described by Kühl *et al.* (1994b). This coefficient is defined as the rate of change of ln-transformed radiance values with depth (Kirk, 1994):

$$K_L = \frac{-\delta(\ln L)}{\delta z} \quad (1)$$

where L represents the field radiance and z the depth. Functions (7th- or 8th-order polynomia) were fitted to the ln-transformed radiance profiles. Hence, the depth profiles of attenuation coefficients (K_L) were calculated from the first derivative with respect to depth of these polynomia.

Microelectrodes. Oxygen was measured using a Clark-type oxygen microelectrode with a guard cathode (Revsbech, 1989). The 90 % response time was <1 s and the stirring sensitivity <1 %. The electrodes had a tip diameter of 10–20 μm. The electrodes were connected to a picoammeter and a recorder. Electrode response was linear and for each profile a two-point calibration was performed in air-saturated medium and anoxic sediment, respectively.

Dissolved hydrogen sulphide was measured with a new amperometric H_2S microelectrode (Jeroschewski *et al.*, 1996; Kühl *et al.*, 1998). The electrodes had a tip diameter of 10–20 μm, a stirring sensitivity of <1–2 % and a 90 % response time <1–2 s. The measuring circuit was composed of a picoammeter using a polarization voltage of +85 mV. Calibrations were performed in a dilution series of a sulphide standard solution buffered with phosphate (0·3 M) to pH 7·8–7·9 and a salinity of 35‰. The calibration procedures were as described in Kühl & Jørgensen (1992b). The total sulphide concentration was determined by the methylene blue technique (cf. Trüper & Schlegel, 1964). When the pH profiles showed a significant variation ($>0·1$ pH unit) from the pH used for the calibration, it was necessary to correct the measured sulphide profiles for this pH variation. The total sulphide concentration, S_t ($S_t = [H_2S] + [HS^-] + [S^{2-}]$), in a solution can be expressed as follows (Stumm & Morgan, 1981):

$$S_t = [H_2S]\left(1 + \frac{K_1}{a_{H^+}} + \frac{K_1K_2}{a_{H^+}^2}\right) \quad (2)$$

where K_1 and K_2 are the first and second dissociation constants of the sulphide equilibrium system, respectively, $[H_2S]$ is the concentration of dissolved hydrogen sulphide, and a_{H^+} is the hydrogen ion activity. The following dissociation constants for sulphide were used: $pK_1 = 7·05$ (Millero *et al.*, 1988) and $pK_2 = 17·1$ (Meyer *et al.*, 1983). The calibration curve for total sulphide determined at a fixed pH of 7·8–7·9 was transformed into a new calibration curve for $[H_2S]$ using equation 2. From this curve it was possible to convert the electrode readings at each pH value to actual H_2S concentration. The total sulphide concentration, S_t, in the pore water could then be calculated from equation 2 by using the actual pH value measured at the same position in the biofilm. The total amount of dissolved H_2S, HS^- and S^{2-} will be designated S_t or sulphide in the rest of the paper.

A glass pH microelectrode (Revsbech & Jørgensen, 1986) connected to a high-impedance millivoltmeter with a calomel electrode (Radiometer) as a reference was used to measure pH. The electrodes were calibrated at different pH values in 0·2 M phosphate-buffered solutions containing 35 g NaCl l^{-1} at room temperature (20 °C). The pH microelectrode had a log-linear response for H^+ and the calibration curves exhibited a slope of 53–58 mV per pH unit and a 90 % response time of <10–20 s.

Measurements were made with a pH and a sulphide microelectrode mounted on the same manually operated micromanipulator (Märtzhaüser). The tips of the pH and sulphide electrode were positioned <2 mm apart in the same horizontal plane. The oxygen microelectrode was mounted in a separate manually operated micromanipulator. All measurements were made in the same 1 cm^2 of the sediment area with a vertical depth resolution of 100 μm.

Calculations of solute fluxes and metabolic processes. Molecular diffusion flux rates were calculated and the depth distribution of metabolic processes was inferred from steady-state oxygen and sulphide profiles.

The one-dimensional diffusion flux of a solute, $J(x)$, is given by Fick's first law of diffusion applied to sediment (Berner, 1980):

$$J(x) = \phi D_s \frac{\delta C(x)}{\delta x} \quad (3)$$

where ϕ is the porosity, D_s the apparent diffusion coefficient of the sediment and C the solute concentration at position x. The ϕD_s values used were calculated as described by Pringault *et al.* (1996); they were $0·694 \times 10^{-5}$ cm^2 s^{-1} and $0·528 \times 10^{-5}$ cm^2 s^{-1} for oxygen and sulphide, respectively. The oxygen flux was calculated from the gradient across the sediment–water interface as described by Rasmussen & Jørgensen (1992). The sulphide flux was calculated from the linear part of the sulphide profile.

P. aestuarii strain CE 2401 was cultured in the BGC for 5 weeks. Microsensor measurements were performed at the end of the culture period. The closed system was opened to allow the insertion of optical and chemical microsensors. Microscopic observations revealed that the possible contamination of the system due to the opening was negligible after a measurement period of 48 h. Profiles of oxygen, sulphide and pH were measured at the end of both the 16 h light and the 8 h dark periods, without interruption of the illumination regime employed during cultivation. After these measurements were completed, an extra series of experiments was performed to study sulphide oxidation. Short-term sulphide and pH dynamics were followed during experimental dark–light shifts using light/dark cycles of much shorter periods, but with the same illumination intensity as used during cultivation. A H_2S and a pH electrode were positioned at the same depth and the two signals were monitored over time. Between successive measurements at different depths, sufficiently long dark periods were allowed to re-establish steady-state dark con-

ditions. Subsequently, anoxygenic photosynthesis of the biofilm as a whole was also studied as a function of illumination intensity in short-term experiments. The sulphide oxidation rate was quantified from the difference of the sulphide influx into the biofilm from below and the efflux of sulphide from the top of the biofilm. This rate was related to the scalar irradiance (430–830 nm) measured at the top of the biofilm (i.e. at 2·2 mm). These measurements were performed after a steady-state was achieved at the illumination intensity studied.

RESULTS

Biofilm development and physico-chemical microenvironment

A biofilm of *Prosthecochloris aestuarii* strain CE 2401 was obtained after 5 weeks incubation. Microscopic observations revealed only cells with the unique morphology of *Prosthecochloris*, indicating that axenic conditions had been maintained throughout the incubation period.

The depth-location of pigment-containing cells was traced from the attenuation of backscattered radiance. *P. aestuarii* contains different bacteriochlorophyll *c* (Bchl *c*) allomers, the carotenoid chlorobactene and minor amounts of bacteriochlorophyll *a* (Bchl *a*). Radiance attenuation peaked at a depth of 2·9–3·0 mm; the attenuation spectrum for this depth layer is shown in Fig. 1(a). The attenuation coefficient K_L at 2·9–3·0 mm shows a maximum around 750 nm with clear shoulders at 675 and 800 nm. The maximum at 750 nm corresponds to the *in vivo* absorption maximum of Bchl *c* (Imhoff, 1995), and the shoulder at 800 nm corresponds to Bchl *a* (Imhoff, 1995). The significant attenuation between 640 and 690 nm showing up as a shoulder around 675 nm can be attributed to bacteriophaeophytin *c* (Bphaeo *c*) (absorption maximum at 670 nm) or to monomeric Bchl *c* (Feiler & Hauska, 1995; Olson, 1981). These compounds may arise in cultures from oligomeric Bchl *c* membrane complexes.

Fig. 1(b) shows radiance attenuation profiles for selected wavelengths, i.e. 750 nm (Bchl *c*), 800 nm (Bchl *a*), 675 nm (as an indicator for Bphaeo *c* and/or monomeric Bchl *c*), and 880 nm as a reference wavelength showing no specific absorption by a liquid *P. aestuarii* culture. The corresponding profiles of the radiance attenuation coefficients (K_L) are shown in Fig. 1(c). From the sediment surface down to 2 mm depth these coefficients were approximately 1 mm^{-1} for all wavelengths, which corresponded to the value found in the unpopulated sediment (data not shown). From 2·2 to 3·5 mm the radiance attenuation coefficients for 675, 750 and 800 nm were significantly higher, but the value for 880 nm remained quite similar. K_L values peaked at 2·9 mm, reaching values of 9·8 mm^{-1} and 7·9 mm^{-1} for 750 nm (Bchl *c*) and 675 nm, respectively. The K_L for 800 nm (Bchl *a*) showed a peak of 5·8 mm^{-1} that was shifted to a lower depth of 3·2 mm. Using K_L for 750 nm as a proxy for *P. aestuarii*, we conclude that the biofilm occupied the depth horizons between 2·2 and 3·5 mm and that its density peaked at 2·9 mm depth. The gap between the attenuation maxima for Bchl *c* (750 nm) and Bchl *a* (800 nm) indicates that, in the biofilm, the ratio Bchl *a*/Bchl *c* increased with depth.

The spectrum of backscattered radiance attenuation coefficients at 3·2–3·3 mm depth is compared with the above-mentioned spectrum at 2·9–3·0 mm depth in Fig. 1(a). The spectrum of K_L at 3·2–3·3 mm depth, below the biofilm maximum, shows a broad peak between 630 and 700 nm and a clear peak at 800 nm showing the enrichment of BChl *a*. In this depth layer 750 nm radiance was depleted to approximately 0·01% of the surface value.

Depth profiles of oxygen, sulphide and pH were measured at the end of the light and dark periods. These profiles are shown in Fig. 2 along with the K_L profile at 750 nm, which visualizes the depth distribution of the biofilm. The maximal oxygen penetration depth was 1·7 mm and 2·2 mm at the end of the dark and light periods, respectively. Sulphide reached the sediment surface at the end of the dark period, and oxygen and sulphide coexisted in the top 1·7 mm (Fig. 2a). Conversely, at the end of the light period sulphide was detectable only below 3 mm. This important shift-down of the sulphide front (i.e. the highest sediment horizon at which sulphide was detected) was due to the photosynthetic sulphide oxidation by the bacteria. As a result, a zone without oxygen and sulphide was located between 2·2 and 3 mm (Fig. 2b).

The downward fluxes of oxygen were 0·045 μmol cm^{-2} h^{-1} and 0·019 μmol cm^{-2} h^{-1} at the end of the dark and light periods, respectively. The corresponding upward sulphide fluxes were substantially higher, viz. 0·131 μmol cm^{-2} h^{-1} and 0·163 μmol cm^{-2} h^{-1} at the end of the dark and light periods, respectively. During the light period, all sulphide diffusing upwards was consumed in the anoxic zone of the sediment, i.e. due to anoxygenic photosynthesis within the *P. aestuarii* biofilm. In contrast, at the end of the dark period, a substantial part (about 50%) of the sulphide diffusing upwards was not consumed in the sediment and escaped into the water column. The rest was oxidized in the oxygen–sulphide coexistence zone, which was located above the *P. aestuarii* biofilm. However, exact budget calculations were not possible, because the profiles were not totally in steady state during the dark period.

At the end of the 8 h dark period, the pH value was 8·3 at the sediment surface in the dark, and slowly decreased with depth, reaching 7·9 at 3 mm. In the light, the pH was almost constant at 8·3 in the top 1 mm of the sand, then increased to pH 9 at 3 mm and decreased again below this peak to 8·5 at 5 mm depth. The maximal pH was located in the sulphide oxidation zone.

Scalar irradiance

The vertical distribution of scalar irradiance is shown in Fig. 3. From 450 to 830 nm the scalar irradiance was strongly attenuated in the sediment (Fig. 3a). Between

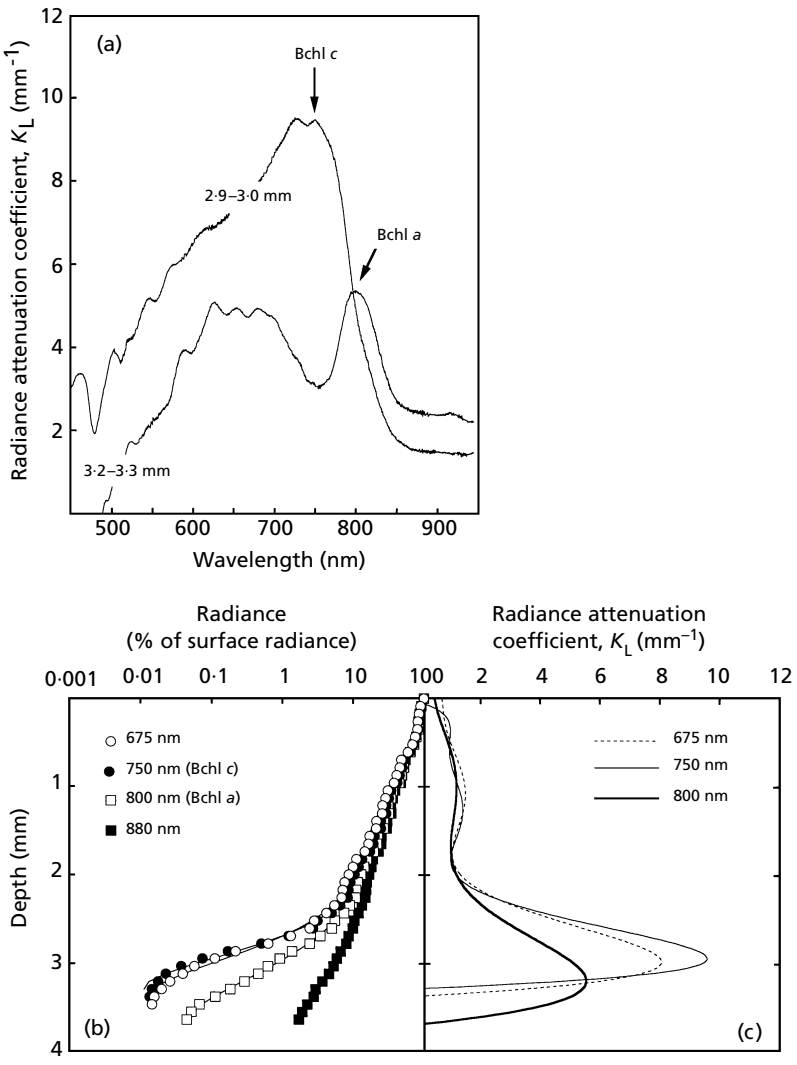

Fig. 1. Backscattered radiance (150°) in a biofilm of *P. aestuarii* strain CE 2401 cultured in the BGC. (a) Spectra of radiance attenuation coefficients (K_L) in different depth layers. (b) Depth profiles of backscattered radiance at selected wavelengths (as indicated corresponding to *in vivo* absorption maxima of the major photopigments in the biofilm). Solid lines represent 7th-order polynomia fitted to the data. (c) Depth profiles of radiance attenuation coefficients (K_L) for the selected wavelengths.

830 and 1000 nm, the attenuation of scalar irradiance was much lower. At the top of the biofilm (2·2 mm depth), integral scalar irradiance comprised 6 μmol photons m^{-2} s^{-1} for 430–550 nm photons and 202 μmol photons m^{-2} s^{-1} for 650–830 nm photons, which can be absorbed by carotenoids and bacteriochlorophylls, respectively. The corresponding values at 3 mm depth, just below the maximum bacterial density, were 1 μmol photons m^{-2} s^{-1} and 45 μmol photons m^{-2} s^{-1} for 430–550 nm and 650–830 nm scalar irradiance, respectively. The effect of the *P. aestuarii* biofilm on the attenuation of scalar irradiance is visualized by comparison with the unpopulated control in Fig. 3(b). Down to 2 mm depth, scalar irradiance was the same under both conditions. Below this depth, significant differences were observed due to the presence of photopigments in the *P. aestuarii* biofilm. Maximal attenuations were observed for photons of wavelengths absorbed by Bchl *c* (750 nm). The attenuation of 675 nm photons was only slightly less than that of 750 nm photons. Photons of 800 nm absorbed by Bchl *a* were also strongly attenuated.

Sulphide oxidation in the biofilm

Vertical oxygen and sulphide profiles showed that at the end of the 16 h light period, oxygen and sulphide were not detectable between 2·2 and 3 mm depth (Fig. 2). To characterize the dynamics of the sulphide pool, dark–light shift experiments were performed at different depths (Fig. 4).

At 1·5 mm depth, the switch-on of the light was not immediately followed by a decrease of sulphide concentration: a lag of 5 min was observed (Fig. 4a). The pH increased 10 min after the switch-on of the light. Sulphide was totally depleted at this depth after 34 min. At 3·0 mm depth, a rapid decrease of sulphide with a substantial increase of pH followed, without lag, the switch-on of light (Fig. 4b). The sulphide decrease was biphasic and comprised an initial rapid decrease during the first 10 min, followed by a slower and linear decrease. Sulphide was totally depleted after 3 h (185 min). The pH was 8·8 after 60 min and remained stable even after depletion of sulphide. At $t = 210$ min the light was switched off; thus, photosynthetic sulphide oxidation

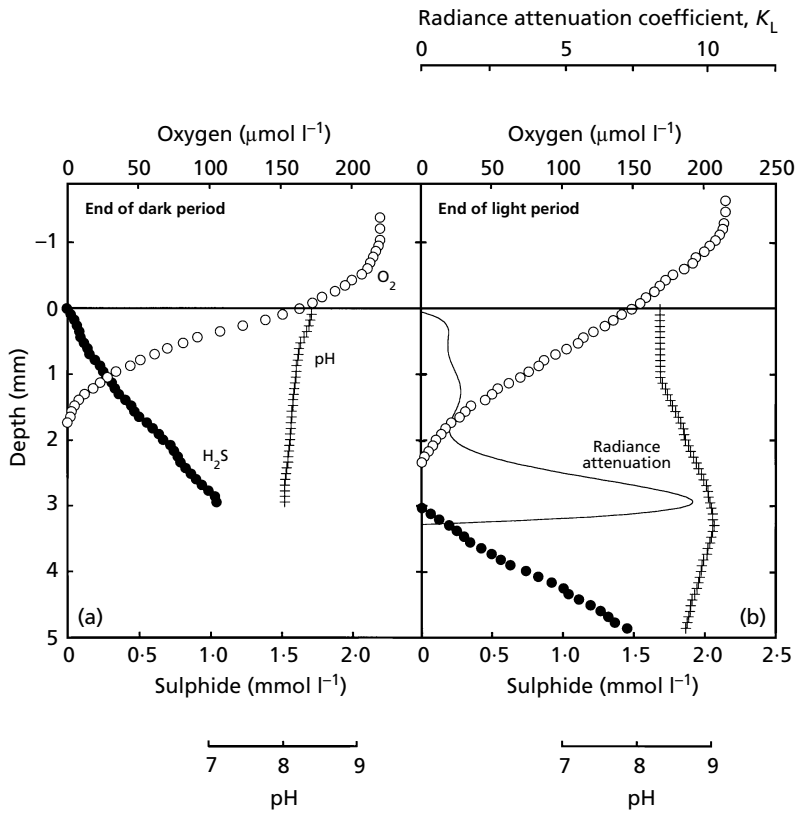

Fig. 2. Oxygen (○), sulphide (●) and pH ( ) profiles in the biofilm of *P. aestuarii* strain CE 2401 cultured in the BGC. The radiance attenuation coefficient profile for 750 nm is depicted as a proxy for the depth distribution of the *P. aestuarii* cells (see text).

stopped. The pH decreased, sulphide reappeared immediately and its concentration increased steadily.

To study the dependence of the rate of sulphide oxidation in the *P. aestuarii* biofilm on the light conditions, measurements were performed at different incident radiation intensities. Sulphide oxidation was measured from steady-state sulphide profiles achieved after long illumination periods. Scalar irradiance was integrated between 430 and 830 nm, and calculated for a depth of 2·2 mm (the upper surface boundary of the biofilm). The sulphide oxidation rate is depicted as a function of scalar irradiance at 2·2 mm depth in Fig. 5. Considering that *P. aestuarii* strain CE 2401 is only able to grow phototrophically, sulphide oxidation for dark (scalar irradiance = 0) was assumed to be equal to zero. The fitted curve was obtained using the hyperbolic model (Jassby & Platt, 1976). The saturation scalar irradiance, E_{0k}, calculated as described by Kirk (1994) was 2 μmol photons m^{-2} s^{-1}.

DISCUSSION

Using the BGC culturing device, an axenic biofilm of *P. aestuarii* strain CE 2401 was obtained in light, oxygen, sulphide and pH gradients within fine sandy sediment simulating benthic growth conditions. *P. aestuarii* strain CE 2401 is nonmotile. At the start of the incubation period, a tiny amount from a batch culture was inoculated throughout the top centimetre of the sediment core. Hence, the bacteria only proliferated where physicochemical conditions were favourable, thus resulting in the biofilm obtained after 5 weeks of incubation. The depth location of the biofilm and its metabolic activities were studied with different optical and chemical microsensors.

Methodology to trace the depth distribution of the biofilm

So far, all efforts to core the sediment in the BGC have not yielded any undisturbed cores, owing to the weak cohesion of the sand. Therefore, it was not possible to obtain a high-resolution depth profile of a biomass parameter like protein or cell number. Nevertheless, the use of radiance microprobes allowed the depth distribution of biomarker photopigments to be traced at a very good spatial resolution (< 100 μm). The attenuation in the biofilm was maximal for wavelengths corresponding to maxima of the *in vivo* absorption spectrum of the organism as previously determined in liquid culture. Thus, the profile of the attenuation coefficient of 750 nm backscattered light (Bchl *c*) provides a proxy of the depth distribution of the phototrophic biofilm. However, a direct conversion of radiance attenuation to biomass is still problematic. Firstly, the spectrum of the attenuation coefficient cannot be quantitatively converted to an absorption spectrum because it requires a knowledge of the length of the optical trajectories of photons in the different layers (Kühl & Jørgensen, 1994). Secondly, the specific contents of the biomarker pigments are not constant,

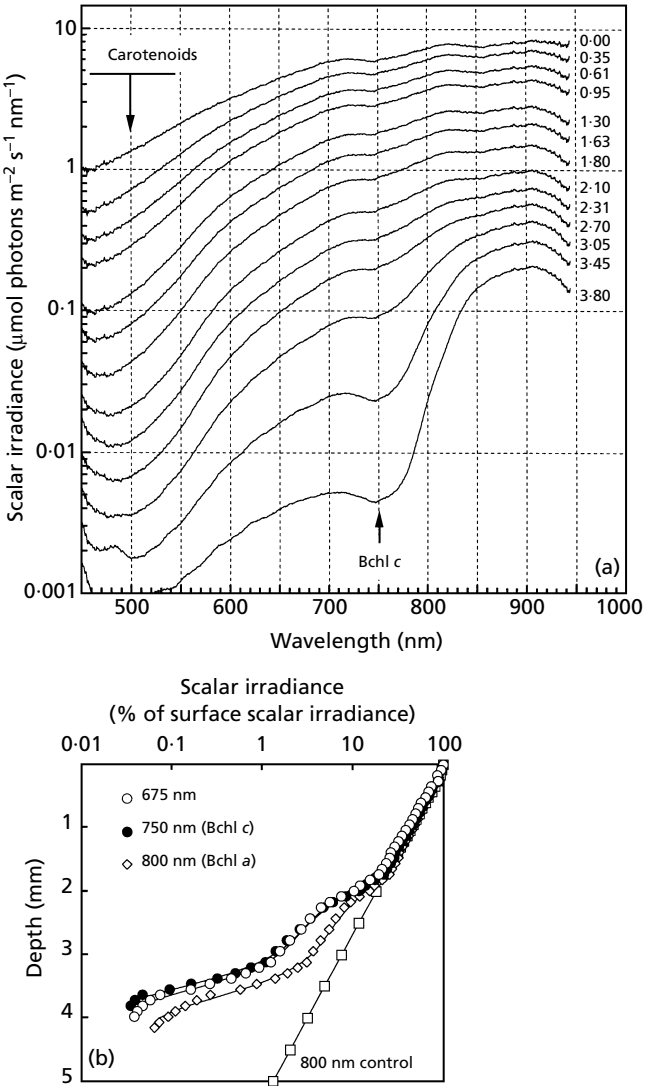

Fig. 3. Scalar irradiance distributions in the biofilm of *P. aestuarii* strain CE 2401 cultured in the BGC. (a) Scalar irradiance spectra from selected depths below the sediment surface (depths in mm are indicated by numbers on the traces). (b) Depth profiles of scalar irradiance attenuation coefficients for wavelengths corresponding to *in vivo* absorption maxima of the major photopigments in the biofilm. The depth profile of 800 nm scalar irradiance in the unpopulated control is presented for comparison.

but rather adapt as a function of irradiance (see Van Gemerden & Mas, 1995, for a review).

The location of the phototrophic biofilm was roughly confirmed by measurements of sulphide oxidation with the chemical sensors using dark–light shift experiments (Fig. 4). In fact, when pH and sulphide microelectrodes were inserted at 1·5 mm, the switch-on of light was not immediately followed by a decrease of the sulphide concentration and an increase of pH. The observed time lag demonstrated that the measurements were not performed directly within the biofilm. Conversely, when the two electrodes were located at the calculated

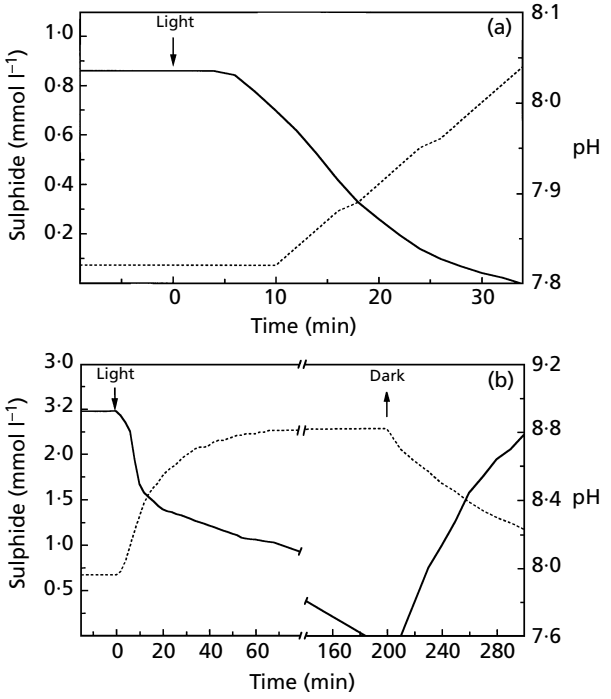

Fig. 4. Time course of sulphide concentrations (solid lines) and pH (dotted lines) during short-term dark–light shift experiments at two different depths (a, 1·5 mm; b, 3·0 mm) within the biofilm of *P. aestuarii* strain CE 2401 cultured in the BGC. Note the discontinuity and difference in scale of the time axis in (b). ↓ indicates when the light is turned on, ↑ when the light is turned off.

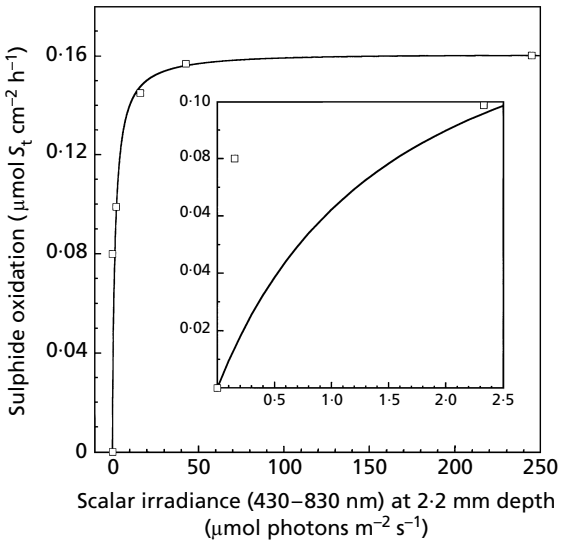

Fig. 5. Sulphide oxidation in a biofilm of *P. aestuarii* strain CE 2401 cultured in the BGC as a function of scalar irradiance at 2·2 mm depth. The solid line represents a curve fit of the hyperbolic function (Jassby & Platt, 1976). The sulphide oxidation in the dark (scalar irradiance = 0) was assumed to be equal to zero as the metabolism of *P. aestuarii* strain CE 2401 is strictly photolithotrophic. The inset shows a more detailed picture of the same data set in the low-light region of the sulphide oxidation versus scalar irradiance plot.

maximal density within the biofilm (i.e. at 3 mm, the depth of maximal radiance attenuation), the sulphide decrease and pH increase followed without delay upon switch-on of light. The initial high rate of sulphide disappearance indicated a very high activity.

Factors limiting the growth of the *P. aestuarii* biofilm

The backscattered radiance profiles showed that the 1·5 mm thick Bchl *c*-containing biofilm was located below 2·2 mm, which is the maximal oxygen penetration depth (Fig. 2). This is clearly due to the fact that growth of *P. aestuarii* strain CE 2401 is entirely inhibited by oxygen (Guyoneaud, 1996; Guyoneaud *et al*., 1996), as is common for all green sulphur bacteria (Van Gemerden & Mas, 1995). *P. aestuarii* strain CE 2401, by not tolerating oxygen, is also not able to grow chemotrophically with sulphide as electron donor and oxygen as electron acceptor. In contrast, this metabolism has been demonstrated for several species of purple sulphur bacteria (Kämpf & Pfennig, 1980; de Wit & Van Gemerden, 1987; Overmann & Pfennig, 1992). During the dark period, oxygen and sulphide coexisted above the biofilm of *P. aestuarii* from 0 to 1·7 mm in high concentrations (e.g. 0·3 mM sulphide with 30 μM oxygen at 1 mm). At the end of the dark period, it was observed that sulphide reached the sediment surface and diffused from the sediment into the water column, clearly showing the imbalance between sulphide oxidation and inputs through diffusion. Due to the absence of sulphide oxidation by bacterial chemosynthesis, the only possible oxidation route for sulphide is the abiotic reaction with oxygen, which is a rather slow process (Millero, 1991). Hence, the abiotic mechanism could not equilibrate the high rate of the sulphide flux.

In contrast, when the purple sulphur bacterium *Thiocapsa roseopersicina* strain EP 2204 was cultured in the BGC under similar conditions for the same incubation period, it was shown that sulphide oxidation was in equilibrium with diffusive delivery after 4 h of darkness and that sulphide never reached the sediment surface. In the reaction zone oxygen and sulphide coexisted in low concentrations only, thus indicating fast oxidation kinetics that was attributed to chemotrophic sulphide oxidation (Pringault *et al*., 1996). In conclusion, the *P. aestuarii* biofilm only consisted of pigment-containing photosynthetically active cells below the maximal oxygen penetration depth.

The turnover of sulphide due to abiotic oxidation is faster at high oxygen and low sulphide concentrations (Millero, 1986). Thus, the abiotic sulphide oxidation cannot be modelled as zero-order kinetics with regard to depth. Due to the slow reaction rate, oxygen penetrates relatively deep into the sediment (2·2 mm in the light), thereby pushing the anaerobic development of the biofilm to lower depths. The imbalance between abiotic sulphide oxidation and influxes generates the formation of intermediate oxidation products, e.g. sulphite (Millero, 1991), which might limit the growth of *P. aestuarii* due to their toxicity.

The axenic biofilm of *P. aestuarii* strain CE 2401 induced a significant increase of pH during the light period, indicating that carbon dioxide fixation was coupled to incomplete sulphide oxidation, with elemental sulphur as the product. Accordingly, the pH reached 9·0 at 3 mm at the end of the light period. During darkness, the pH decreased and pH values in the biofilm stabilized at 7·9. High pH values in the BGC might be inhibitory for growth of this species, which is optimal at pH 6·7 (Guyoneaud, 1996).

Growth and light conditions

The biofilm of *P. aestuarii* strain CE 2401 was entirely phototrophic, meaning that radiation was the sole energy source. Therefore, scalar irradiance is an essential factor which governs growth and survival. The scalar irradiance at the sediment surface comprised 800 μmol photons m^{-2} s^{-1} and 2200 μmol photons m^{-2} s^{-1} for PAR (430–700 nm) and NIR (700–1000 nm), respectively. The scalar irradiance for the PAR was two times lower than natural light conditions in very sunny environments, where microbial mats with green sulphur bacteria like *P. aestuarii* occur (Pierson *et al*., 1990). However, qualitatively, the radiation used in the BGC was enriched in NIR light, favouring the development of anoxygenic phototrophic bacteria. Moreover, the scalar irradiance attenuation in the non-inoculated reconstituted sediments was low (K_{NIR} 0·95 mm^{-1}) compared to wet sand (K_{NIR} 1·2 mm^{-1}) with the same granulometry sampled from the natural environment (Kühl *et al*., 1994a). Scalar irradiance of NIR photons at 3 mm still represented 10 % of the surface value at the start of the incubation (Fig. 3b). Thus, the NIR scalar irradiance at this depth was 220 μmol photons m^{-2} s^{-1}, which is largely sufficient for growth of green sulphur bacteria (Van Gemerden & Mas, 1995).

During the incubation time, the scalar irradiance decreased in the biofilm due to the biosynthesis of photopigments. As a result, after 5 weeks of incubation the scalar irradiance for NIR at 3 mm depth represented only 3 % of the surface value. The attenuation of scalar irradiance was maximal for 750 nm, which corresponds to the *in vivo* Bchl *c* absorption maximum. The flux density of photons in the biofilm can be directly compared with the diffusive flux of sulphide by recalculating the fluxes of photons to the same dimensions as used for the chemical flux. Hence, on the top of the biofilm (2·2 mm) the photon scalar irradiance comprised 2·2 μmol photons cm^{-2} h^{-1} (430–550 nm photons) and 72 μmol photons cm^{-2} h^{-1} (650–830 nm photons), which can be absorbed by the carotenoids and the bacteriochlorophylls, respectively. The corresponding values at 3 mm depth just below the maximum were 0·36 μmol photons cm^{-2} h^{-1} and 16·2 μmol photons cm^{-2} h^{-1} for 430–550 nm and 650–830 nm, respectively. The diffusive delivery of sulphide towards the biofilm was 0·16 μmol cm^{-2} h^{-1}. It has been shown that the fixation of 1 mol C in green sulphur bacteria requires roughly 4 (3·3–4·5) mol photons (Brune, 1989), which corresponds to 2 or 0·5 mol sulphide consumed, dependent on the

sulphide being oxidized to sulphur or sulphate, respectively. Thus 0·16 mol sulphide oxidized corresponds roughly to 0·32–1·28 mol photons absorbed.

Accordingly, it appears that scalar irradiance on top of the biofilm was largely sufficient to cope with the diffusive sulphide flow. Therefore, sulphide oxidation rates in the top part of the biofilm exceeded the diffusive delivery. Sulphide oxidation in the top layers only took place during a short transient period upon the switch-on of the light, while the sulphide front shifted downwards and stabilized at 3 mm. Even at 3 mm depth the photon flux density exceeded the diffusive flow of sulphide by a factor of 10 or more. However, photons are also harvested for maintenance which is not coupled to sulphide oxidation, and the probability of photon absorption is lower than one. Thus light limitation at 3 mm depth cannot be excluded, since scalar irradiance sustained a rate of sulphide oxidation that was balanced by diffusive delivery of sulphide.

The probability of harvesting photons of different wavelengths is biologically determined by the *in vivo* absorption spectrum, which is a function of the specific pigment contents and their spatial and biochemical organization in the cells. A proxy of the *in vivo* absorption spectra of *P. aestuarii* strain CE 2401 in the biofilm is given by the corresponding spectra of backscattered attenuation coefficients, but comparisons should be made with care due to the problematic conversion between attenuation and absorption (see above). The attenuation spectrum in the peak of the biofilm (2·9–3 mm) showed a maximum of around 750 nm as expected, with shoulders at 650–675 nm and at 800 nm (Fig. 1a). The shoulder at 800 nm is due to Bchl *a* molecules that occupy an intermediate position in the energy transfer from the Bchl *c* antennae molecules in the chlorosomes into the Bchl *a* in the reaction centre (Freiberg *et al*., 1988; Blankenship *et al*., 1995). Potentially these include both membrane-bound Bchl *a* molecules in the chlorosome baseplate (absorption maximum 795 nm) (Blankenship *et al*., 1995) and the protein-bound Bchl *a* molecules in the Fenna–Mathews–Olson (FMO) protein, which has a maximum absorption at 808–809 nm (Blankenship *et al*., 1995; Olson, 1978). The Bchl *a*-containing reaction centre has an *in vivo* absorption maximum at around 840 nm. The latter is not discernible from the attenuation spectrum, which is normal for green sulphur bacteria due to the low amounts of Bchl *a* present in the reaction centre. The importance of the 800 nm Bchl *a*-dependent absorption was enhanced at 3·2–3·3 mm, where 750 nm scalar irradiance was depleted below 0·01% of the surface value. This could indicate that, in the deep biofilm, the bacterium synthesized relatively more Bchl *a* molecules functioning in the chlorosome baseplate as antennae at around 800 nm, probably as a chromatic adaptation to the prevailing light climate. Typical Bchl *a*/Bchl *c* ratios in *Chlorobiaceae* are around 1:10 to 1:20 (Gorlenko, 1988; Pierson & Castenholz, 1978), but a low ratio of approximately 1:3 has been found in some strains (Freiberg *et al*., 1988).

The shoulder around 675 nm can be attributed to Bphaeo *c* or to monomeric Bchl *c*. Recently, it has been found that Bphaeo *c* is formed from Bchl *c* (loss of Mg^{2+}) in cultures of *Chlorobium tepidum* during the stationary phase and that energy transfer is possible from Bphaeo *c* to Bchl *c* and subsequently through baseplate and FMO Bchl *a* into the reaction centre (Tokita *et al*., 1997). However, a possible occurrence of Bphaeo *c* requires chemical verification and its potential role in the biofilm remains unknown.

Irradiance response curve of anoxygenic photosynthesis

The relation between carbon dioxide fixation or photosynthetic oxygen production and available radiant energy has been studied extensively for oxygenic photosynthesis both in cultures and in field samples (Kirk, 1994). In contrast, concerning anoxygenic photosynthesis, only a few studies have been performed, and these were based mostly on phototrophic bacteria cultured in liquid media (Overmann *et al*., 1992; Van Gemerden, 1980; Veldhuis & Van Gemerden, 1986). In this study the relation between scalar irradiance (450–830 nm) at the top of the *P. aestuarii* biofilm (2·2 mm) and the sulphide oxidation rate was quantified by varying the illumination intensity (Fig. 5). The saturation scalar irradiance for the biofilm (E_{0k}) was 2 μmol photons m^{-2} s^{-1}; this value is comparable to the E_{0k} measured in liquid cultures of *Chlorobium phaeobacterioides* strain MN1, which was isolated from extremely low-light environments (Overmann *et al*., 1992).

However, the response curve of the biofilm (Fig. 5) cannot be considered as the specific *P* versus *I* curve (photosynthesis versus scalar irradiance) for *P. aestuarii* strain CE 2401, for the following reasons. Firstly, because the maximum sulphide oxidation rate observed in the biofilm (0·161 μmol S_t cm^{-2} h^{-1}) was imposed by the diffusive sulphide flux (0·163 μmol S_t cm^{-2} h^{-1}). This limitation pushes the E_{0k} to lower scalar irradiance values. Secondly, because a strong scalar irradiance gradient occurred throughout the biofilm. As a result, at low light intensities most of the sulphide was oxidized in the top part of the biofilm. At higher light intensities the sulphide front shifted downwards and, consequently, sulphide was oxidized in the deeper parts of the biofilm. The scalar irradiance (245 μmol photons m^{-2} s^{-1}) on top of the biofilm during cultivation was much higher than the steady-state saturation intensity ($E_{0k} = 2$ μmol photons m^{-2} s^{-1}) for sulphide oxidation. This showed that the biomass yield after 5 weeks of incubation was limited by the diffusive flux of sulphide and not by scalar irradiance penetrating into the anoxic sediment layers.

Ecological aspects

The cultivation of *P. aestuarii* strain CE 2401 in a gradient system allowed us to study factors controlling its growth in benthic gradients. An axenic biofilm was obtained and its location in the sediment confirmed that

the bacterium grows only in anoxic layers. The experimental biofilm is not directly comparable to the green layer of *P. aestuarii* in the multi-layered mats described by Pierson *et al.* (1987). The cyanobacteria in the top mat, by producing oxygen, push *Prosthecochloris* downwards to 6–7 mm depth (Nicholson *et al.*, 1987). The available irradiance (Pierson *et al.*, 1990) was lower than in the BGC culture; the bacteria probably compensate by a high affinity for the light. In our study, the biomass yield of *P. aestuarii* was not limited by light but rather by the sulphide influx. Alkaline conditions in the BGC were due to CO_2 fixation and incomplete sulphide oxidation by *P. aestuarii* strain CE 2401. However, in its natural environment heterotrophic bacteria produce acids, thereby contributing to the maintenance of a neutral pH, which is more favourable for the growth of green sulphur bacteria.

ACKNOWLEDGEMENTS

Olivier Pringault thanks Professor Bo Barker Jørgensen and Professor Friedrich Widdel for the possibility to stay at the Max Planck Institut für Marine Mikrobiologie (Bremen, Germany) during a period of 4 months. Helle Ploug is thanked for her help with the calibration procedures of the scalar irradiance measurements. John Ormerod and Mette Miller are thanked for stimulating discussions and comments. The technicians of the Microsensor Research Group of the MPI, particularly Gaby Eickert, are thanked for their efforts with microsensor construction. Olivier Pringault was supported by fellowships from the French Ministry of Higher Education and Research (MESR) and from the Deutscher Akademischer Austausschdienst (DAAD). Part of this study was supported by the Red-Sea Research Programme, Project E 'Microbial activities in hypersaline interfaces controlling nutrient fluxes', financed by the German Ministry for Research and Development (BMBF).

REFERENCES

Berner, R. J. (1980). *Early Diagenesis: a Theoretical Approach*. Princeton, NJ: Princeton University Press.

Blankenship, R. E., Olson, J. M. & Miller, M. (1995). Antenna complexes from green photosynthetic bacteria. In *Anoxygenic Photosynthetic Bacteria*, pp. 399–435. Edited by R. E. Blankenship, M. T. Madigan & C. E. Bauer. Dordrecht: Kluwer.

Brune, D. C. (1989). Sulfur oxidation by phototrophic bacteria. *Biochim Biophys Acta* **975**, 189–221.

Feiler, U. & Hauska, G. (1995). Green sulfur bacterial reaction centers. In *Anoxygenic Photosynthetic Bacteria*, pp. 665–685. Edited by R. E. Blankenship, M. T. Madigan & C. E. Bauer. Dordrecht: Kluwer.

Freiberg, A. M., Timpmann, K. E. & Fetisova, Z. G. (1988). Excitation energy transfer in living cells of the green bacterium *Chlorobium limicola* studied by picosecond fluorescence spectroscopy. In *Green Photosynthetic Bacteria*, pp. 81–90. Edited by J. M. Olson, J. G. Ormerod, J. Amesz, E. Stackebrandt & H. G. Trüper. New York: Plenum.

Garcia, H. E. & Gordon, L. I. (1992). Oxygen solubility in seawater: better fitting equations. *Limnol Oceanogr* **37**, 1307–1312.

Gorlenko, V. M. (1988). Ecological niches of green sulfur and gliding bacteria. In *Green Photosynthetic Bacteria*, pp. 257–267. Edited by J. M. Olson, J. G. Ormerod, J. Amesz, E. Stackebrandt & H. G. Trüper. New York: Plenum.

Guyoneaud, R. (1996). *Etude écologique, physiologique et systématique des communautés de bactéries phototrophes anoxygéniques en milieu lagunaire méditerranéen et atlantique*. PhD thesis, Université Bordeaux I, France.

Guyoneaud, R., Matheron, R., Baulaigue, R., Podeur, K., Hirschler, A. & Caumette, P. (1996). Anoxygenic phototrophic bacteria in eutrophic coastal lagoons of the French Mediterranean and Atlantic Coasts (Prévost Lagoon, Arcachon Bay, Certes Fishponds). *Hydrobiologia* **329**, 33–43.

Imhoff, J. F. (1995). Taxonomy and physiology of phototrophic purple and green sulfur bacteria. In *Anoxygenic Photosynthetic Bacteria*, pp. 1–15. Edited by R. E. Blankenship, M. T. Madigan & C. E. Bauer. Dordrecht: Kluwer.

Jassby, A. D. & Platt, T. (1976). Mathematical formulation of the relationship between photosynthesis and light for phytoplankton. *Limnol Oceanogr* **21**, 540–547.

Jeroschewski, P., Steuckart, C. & Kühl, M. (1996). An amperometric microsensor for the determination of H_2S in aquatic environments. *Anal Chem* **68**, 4351–4357.

Kämpf, C. & Pfennig, N. (1980). Capacity of Chromatiaceae for chemotrophic growth. Specific respiration rates of *Thiocystis violacea* and *Chromatium vinosum*. *Arch Microbiol* **127**, 125–135.

Kirk, J. T. O. (1994). *Light and Photosynthesis in Aquatic Ecosystems*, 2nd edn. Cambridge: Cambridge University Press.

Kühl, M. & Jørgensen, B. B. (1992a). Spectral light measurements in microbenthic phototrophic communities with a fiber-optic microprobe coupled to a sensitive diode array detector. *Limnol Oceanogr* **37**, 1813–1823.

Kühl, M. & Jørgensen, B. B. (1992b). Microsensor measurements of sulfate reduction and sulfide oxidation in compact microbial communities of aerobic biofilms. *Appl Environ Microbiol* **58**, 1164–1174.

Kühl, M. & Jørgensen, B. B. (1994). The light field of microbenthic communities: radiance distribution and microscale optics of sandy coastal sediments. *Limnol Oceanogr* **39**, 1368–1398.

Kühl, M., Lassen, C. & Jørgensen, B. B. (1994a). Light penetration and light intensity in sandy marine sediments measured with irradiance and scalar irradiance fiber-optic microprobes. *Mar Ecol Prog Ser* **105**, 139–148.

Kühl, M., Lassen, C. & Jørgensen, B. B. (1994b). Optical properties of microbial mats: light measurements with fiber-optic microprobes. In *Microbial Mats: Structure, Development and Environmental Significance* (NATO ASI Series, vol. G35), pp. 149–167. Edited by L. J. Stal & P. Caumette. Berlin & Heidelberg: Springer.

Kühl, M., Steuckart, C., Eickert, G. & Jeroschewski, P. (1998). A H_2S microsensor for profiling biofilms and sediments: application in an acidic lake sediment. *Aquat Microb Ecol* (in press).

Lassen, C., Ploug, H. & Jørgensen, B. B. (1992). A fibre-optic scalar irradiance microsensor: application for spectral light measurements in sediments. *FEMS Microbiol Ecol* **86**, 247–254.

Millero, F. J. (1986). The thermodynamics and kinetics of the hydrogen sulfide system in natural waters. *Mar Chem* **18**, 121–147.

Millero, F. J. (1991). The oxidation of H_2S in Framvaren Fjord. *Limnol Oceanogr* **36**, 1007–1014.

Millero, F. J., Plese, T. & Fernandez, M. (1988). The dissociation of hydrogen sulfide in seawater. *Limnol Oceanogr* **33**, 269–274.

Meyer, B., Ward, K., Koshalp, K. & Peter, L. (1983). Second dissociation constant of hydrogen sulfide. *Inorg Chem* **22**, 2345–2346.

Nicholson, J. A., Stolz, J. F. & Pierson, B. K. (1987). Structure of microbial mat at Great Sippewisset Marsh, Cape Cod, Massachusetts. *FEMS Microbiol Ecol* **45**, 343–364.

Olson, J. M. (1978). Bacteriochlorophyll *a*-proteins from green bacteria. In *The Photosynthetic Bacteria*, pp. 161–178. Edited by R. K. Clayton & R. S. Sistrom. New York: Plenum.

Olson, J. M. (1981). Bacteriopheophytin *c* in reaction center complexes of green photosynthetic bacteria. *Biochim Biophys Acta* **637**, 185–188.

Overmann, J. & Pfennig, N. (1992). Continuous chemotrophic growth and respiration of Chromatiaceae species at low oxygen concentrations. *Arch Microbiol* **158**, 59–67.

Overmann, J., Cypionka, H. & Pfennig, N. (1992). An extremely low-light-adapted phototrophic sulfur bacterium from the Black Sea. *Limnol Oceanogr* **37**, 150–155.

Pfennig, N. (1989). Ecology of phototrophic purple and green sulfur bacteria. In *Autotrophic Bacteria*, pp. 97–116. Edited by H. G. Schlegel & B. Bowien. Madison, WI: Science Tech Publishers.

Pfennig, N. & Trüper, H. G. (1992). The family Chromatiaceae. In *The Prokaryotes*, 2nd edn, pp. 3200–3221. Edited by A. Balows, H. G. Trüper, M. Dworkin, W. Harder & K. H. Schleifer. New York: Springer.

Pierson, B. K. & Castenholz, R. W. (1978). Photosynthetic apparatus and cell membranes of green bacteria. In *The Photosynthetic Bacteria*, pp. 179–197. Edited by R. K. Clayton & W. R. Sistrom. New York: Plenum.

Pierson, B. K., Oesterle, A. & Murphy, G. L. (1987). Pigments, light penetration and photosynthetic activity in the multi-layered microbial mats of Great Sippewissett salt marsh. *FEMS Microbiol Ecol* **45**, 365–376.

Pierson, B. K., Sands, V. M. & Frederick, J. L. (1990). Spectral irradiance and distribution of pigments in a highly layered marine microbial mat. *Appl Environ Microbiol* **56**, 2327–2340.

Ploug, H., Lassen, C. & Jørgensen, B. B. (1993). Action spectra of microalgal photosynthesis and depth distribution of spectral scalar irradiance in a coastal marine sediment of Limfjorden, Denmark. *FEMS Microbiol Ecol* **12**, 69–78.

Pringault, O., De Wit, R. & Caumette, P. (1996). A Benthic Gradient Chamber for culturing phototrophic sulfur bacteria on reconstituted sediments. *FEMS Microbiol Ecol* **20**, 237–250.

Rasmussen, H. & Jørgensen, B. B. (1992). Microelectrode studies of seasonal oxygen uptake in a coastal sediment: role of molecular diffusion. *Mar Ecol Prog Ser* **81**, 289–303.

Revsbech, N. P. (1989). An oxygen microsensor with a guard cathode. *Limnol Oceanogr* **34**, 472–476.

Revsbech, N. P. & Jørgensen, (1986). Microelectrodes: their use in microbial ecology. *Adv Microb Ecol* **9**, 293–352.

Stal, L. J., Van Gemerden, H. & Krumbein, W. E (1985). Structure and development of a benthic microbial mat. *FEMS Microbiol Ecol* **31**, 111–125.

Stumm, W. & Morgan, J. J. (1981). *Aquatic Chemistry. An Introduction Emphasizing Chemical Equilibria in Natural Waters*. New York: Wiley.

Tokita, S., Hirota, M., Shimada, K. & Matsuura, K. (1997). Phaeophytinization of bacteriochlorophyll *c* and energy transfer in cells of *Chlorobium tepidum*. In *Book of Abstracts of the IXth International Symposium on Phototrophic Prokaryotes*, *Vienna*, *1997*, p. 112. Edited by G. A. Peschek, W. Löffelhardt & G. Schmetterer.

Trüper, H. G. & Schlegel, H. G. (1964). Sulphur metabolism in Thiorhodaceae. I. Quantitative measurements on growing cells of *Chromatium okenii*. *Antonie Leeuwenhoek* **30**, 225–238.

Van Gemerden, H. (1980). Survival of *Chromatium vinosum* at low light intensities. *Arch Microbiol* **125**, 115–121.

Van Gemerden, H. (1984). The sulfide affinity of phototrophic bacteria in relation to the location of elemental sulfur. *Arch Microbiol* **139**, 289–294.

Van Gemerden, H. (1987). Competition between purple sulfur bacteria and green sulfur bacteria: role of sulfide, sulfur and polysulfides. *Acta Academiae Aboensis* **47**, 13–27.

Van Gemerden, H. (1993). Microbial mats: a joint venture. *Mar Geol* **113**, 3–25.

Van Gemerden, H. & Mas, J. (1995). Ecology of phototrophic sulfur bacteria. In *Anoxygenic Photosynthetic Bacteria*, pp. 49–85. Edited by R. E. Blankenship, M. T. Madigan & C. E. Bauer. Dordrecht: Kluwer.

Van Gemerden, H., Tughan, C. S., De Wit, R. & Herbert, R. A. (1989). Laminated microbial ecosystems on sheltered beaches in Scapa flow, Orkney Islands. *FEMS Microbiol Ecol* **62**, 87–102.

Veldhuis, M. J. W. & Van Gemerden, H. (1986). Competition between purple and brown phototrophic bacteria in stratified lakes: sulfide, acetate and light as limiting factors. *FEMS Microbiol Ecol* **38**, 31–38.

de Wit, R. & Van Gemerden, H. (1987). Chemolithotrophic growth of the phototrophic sulfur bacterium *Thiocapsa roseopersicina*. *FEMS Microbiol Ecol* **45**, 117–126.

Received 29 August 1997; revised 17 November 1997; accepted 2 December 1997.